3D estimation of Direction of Arrival using Uniform Phased Array Antenna on multi-targeting FMCW RADAR

RANDRIANANDRASANA Marie Emile[1], RANDRIAMITANTSOA Paul Auguste[2],
RANDRIAMITANTSOA Andry Auguste[3]

[1] Dept. of Telecommunication, Antsirabe Vankinankaratra High Education Institute,
University of Antananarivo, Madagascar
[2] Dept. of Telecommunication, High School Polytechnic of Antananarivo,
University of Antananarivo, Madagascar
[3] Dept. of Telecommunication, High School Polytechnic of Antananarivo,
University of Antananarivo, Madagascar,

ABSTRACT

Multiple input/multiple output (MIMO) radar system performance benefits from the capability to simultaneously transmit and receive multiple orthogonal waveforms. For pulse radars fitting orthogonal waveforms have been developed. These waveforms are however not necessarily suitable for frequencymodulated continuous-wave (FMCW) radar. The theory of an uniform phased array antenna is used on receiver not on classic transmitter to estimate the direction of angular. Conventional Direction of Arrival (DOA) estimation algorithms, such as Multiple Signal Classification (MUSIC), Root-MUSIC, and Estimating Signal Parameters via Rotational Invariance Techniques (ESPRIT) algorithms, are difficult to apply to large-scale antenna arrays. Because these algorithms not only require a lot of snapshots of the received data, but also the hardware equipment cannot meet the algorithm complexity requirements. In this article, we use double 3D-FFT to estimate the direction of arrival on the Uniform Rectangular Antenna (URA), the velocity and the distance of the target. The major benefit of the FMCW radar principle is that the bandwidth of the beat signal is generally much smaller than the signal bandwidth, relaxing sampling requirements. Combined with 3D estimation, the FMCW could have more precision on estimation of targets.

Keyword : - *MIMO , FMCW, URA, DOA, 3D-FFT*

---

1. INTRODUCTION

By the Maxwell theory, the phased array antenna could be used to beamforming the wave on a specific angular. Multiple antenna shape could be use for it. Combined with FMCW radar we could use it to beam the MIMO Radar.

1.1 Ultra WidebBand Beamforming

UWB or Ultra Wide Band Antenna is a very wide band antenna family from patch antennas. These antennas have particular waveforms in: E, T, H, Vivaldi, Fractal, Log periodic patch These antennas are used for MIMO and BeamForming technology using several uniform antennas (phased arrays antenna).

Phased arrays antenna is a family of antennas grouped for radiation inclined at a well-defined angle according to the phases of the antennas. The possible configuration is:
- Linear: the antennas are arranged in a horizontal line
- Circular: the antennas are arranged in a well-defined circle
- Planar: The antennas are arranged on a well-defined surface.
- Compliant: The antennas are arranged on a well-defined non-planar shape.

1.2 Wave propagation

To be able to intelligently beam a wave beam using multi-antenna systems such as the Phased Arrays Antenna expressed in Formula (1).

$$AP=EF \times AF \qquad (1)$$

AP or Array Pattern is the total propagation emitted by multiple antennas.

EF or Element Fields is the propagation of an individual antenna

AF or Array Factor is the variable geometric propagation (the antenna shape, excitation with amplitude and phase).

Let's start from Maxwell's equation:

$$div(\overline{D}) = \rho \quad ; \quad div(\overline{B}) = 0$$

$$\overrightarrow{rot}(\vec{E}) = -\frac{\partial \vec{B}}{\partial t} \quad ; \quad \overrightarrow{rot}(\vec{H}) = \vec{j} + \frac{\partial \vec{D}}{\partial t}$$

In vacuum, the electric field and the magnetic field are related by the following relations:

$$\overline{D} = \varepsilon_0 \overline{E} \quad ; \quad \overline{B} = \mu_0 \overline{E}$$

Where, $\varepsilon_0 = \frac{1}{36\pi 10^9}$: Dielectric permittivity of vacuum and $\mu_0 = 4\pi 10^{-7}$: Magnetic permeability of vacuum.

Noted $\vec{A}$ a potential vector of a source $\vec{J}$ and ρ :

$$\begin{cases} \nabla \times \vec{E} = -j\omega\mu\overline{H} \\ \nabla\overline{H} = j\omega\varepsilon\vec{E} + \vec{J} \end{cases}$$

$$\nabla.\vec{B} = 0 \text{ , alors } \vec{B} = \nabla \times \vec{A}$$

$$\begin{cases} \vec{E} = -j\omega\vec{A} - \nabla\phi \\ j\omega\varepsilon\vec{E} = \nabla \times \left(\frac{1}{\mu}\nabla \times \vec{A}\right) - \vec{J} \end{cases}$$

ϕ is called a potential scalar. So, we could obtain :

$$\nabla \times \nabla \times \vec{A} + j\omega\mu\varepsilon\left(j\omega\vec{A} + \nabla\phi\right) = \mu\vec{J}$$

with, $\nabla \times \nabla \times = \nabla\nabla. - \nabla^2$ and $\nabla.\vec{A} = -j\omega\mu\phi$

So, $\nabla^2\vec{A} + \beta^2\vec{A} = -\mu\vec{J}$

By posing, $\beta = \omega\sqrt{\mu\varepsilon}$

For the case of a dipole, $\vec{A}$ exists only following the z-axis. So, $\nabla^2\vec{A}_z + \beta^2\vec{A}_z = -\mu\vec{J}$

Using the spherical coordinate, this equation can be reduced to a derivative with a definite r number.

$$\frac{d^2}{dr^2}\vec{A}_z + \frac{2}{r}\frac{dA_z}{dr} + \beta^2\vec{A}_z = 0$$

The solutions of the equation are:

$$\begin{cases} A_{z_1} = \dfrac{C_1 e^{-j\beta r}}{r} \\[2mm] A_{z_2} = \dfrac{C_2 e^{-j\beta r}}{r} \end{cases}$$

By using the initial condition of the differential equation we therefore:

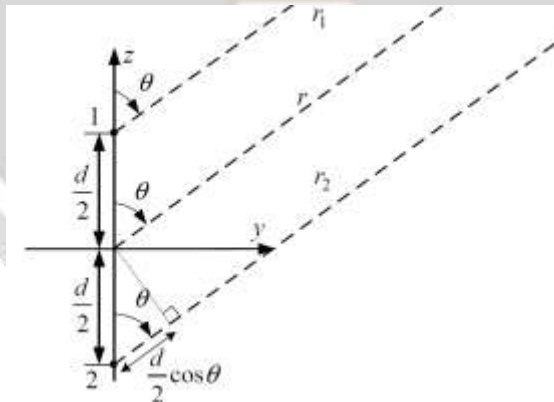$$C_1 = \frac{1}{4\pi}\mu J_z \quad ; \quad A_z = \mu J_z \frac{e^{-j\beta r}}{4\pi}$$

Like, $\vec{H} = \dfrac{1}{\mu}\nabla \times \vec{A}$

Then the electromagnetic field E is of the form :

$$E = \frac{Me^{-jkr}}{4\pi r}$$

Where, M : the magnitude of the wave; k : the proportional to the field frequency E.

Take the following Figure no (1) to demonstrate Formula (1)

Fig -1 : Representation of electromagnetic fields ime latency with QAM

Looking at this figure we see that :

$$E = E_1 + E_2$$

$$E = \frac{M}{4\pi r}\left[e^{-jk\left[r-\frac{d}{2}\cos\theta\right]} + e^{-jk\left[r+\frac{d}{2}\cos\theta\right]}\right]$$

$$E = \frac{M}{4\pi r} e^{-jkr} \left[e^{j\frac{kd}{2}\cos\theta} + e^{-j\frac{kd}{2}\cos\theta} \right]$$

$$E = \underbrace{\frac{M}{4\pi r} e^{-jkr}}_{EF} \underbrace{\left[2\cos\frac{k\cos\theta}{2} \right]}_{AF}$$

2. MATERIALS AND METHODS
2.1. Phased Array Antenna using Uniform Linear Antenna (ULA)

ULA antenna is a family of antenna represented linearly spaced by a uniform distance.
•   ULA relative to the vertical
ULA with uniform amplitude and progressive phase deflects its lobe at an upward angle. The uniform phases must follow the equation:
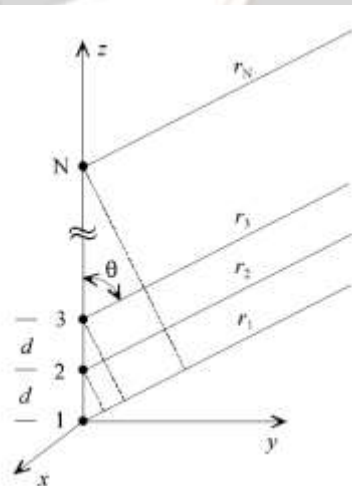
$$\alpha = \frac{\omega d \cos(\theta)}{c} \tag{2}$$

Where, α : the uniform phase; ω : the frequency ; d : the antenna spacing; c : the speed of light ; θ : the angle from vertical

In the Figure 2, each dot $1, 2, \cdots N$ represents an antenna that is uniformly spaced by the distance d .

The propagation equation of an element is defined by:

$$E_\theta = I_0 \frac{e^{-jkr}}{4\pi r}$$

Fig -2 : Representation of Uniform Linear Antenna

In the Figure no 2, we could also constat that :

$$\begin{cases} r_1 = r \\ r_2 \approx r - d\cos(\theta) \\ r_3 \approx r - 2d\cos(\theta) \\ \vdots \\ r_N \approx r - (N-1)d\cos(\theta) \end{cases}$$

The magnitudes for each antenna will therefore be :

$$I_1 = I_0 \quad I_2 = I_0 e^{j\phi_2} \quad I_3 = I_0 e^{j\phi_3} \quad \cdots \quad I_N = I_0 e^{j\phi_N}$$

The propagation of each antenna will therefore be :

$$E_{\theta 1} \approx I_0 \frac{e^{-jkr}}{4\pi r} E_0$$

$$E_{\theta 2} \approx I_0 \frac{e^{-jk(r-d\cos(\theta))}}{4\pi r} E_0 = E_0 e^{j(\phi_2 + kd\cos(\theta))}$$

$$E_{\theta 3} \approx I_0 \frac{e^{-jk(r-2d\cos(\theta))}}{4\pi r} E_0 = E_0 e^{j(\phi_3 + 2kd\cos(\theta))}$$

$$\vdots$$

$$E_{\theta 3} \approx I_0 \frac{e^{-jk(r-(N-1)d\cos(\theta))}}{4\pi r} E_0 = E_0 e^{j(\phi_N + (N-1)kd\cos(\theta))}$$

$$E_\theta = E_{\theta 1} + E_{\theta 2} + E_{\theta 3} + \cdots + E_{\theta N}$$

$$E_\theta = E_0 + E_0 e^{j(\phi_2 + kd\cos(\theta))} + E_0 e^{j(\phi_3 + 2kd\cos(\theta))} + \cdots + E_0 e^{j(\phi_N + (N-1)kd\cos(\theta))}$$

$$E_\theta = E_0 \left[1 + e^{j(\phi_2 + kd\cos(\theta))} + e^{j(\phi_3 + 2kd\cos(\theta))} + \cdots + e^{j(\phi_N + (N-1)kd\cos(\theta))} \right]$$

$$E_\theta = E_0 \times AF;$$

$$AF = \left[1 + e^{j(\phi_2 + kd\cos(\theta))} + e^{j(\phi_3 + 2kd\cos(\theta))} + \cdots + e^{j(\phi_N + (N-1)kd\cos(\theta))} \right]$$

As the phases are also progressive then,

$$\phi_1 = 0 \quad \phi_2 = \alpha \quad \phi_3 = 2\alpha \quad \cdots \quad \phi_N = (N-1)\alpha$$

By inserting the value of the phase in the equation of the AF, we will have :

$$AF = \left[1 + e^{j\Psi} + e^{j(2\Psi)} + \cdots + e^{j((N-1)\Psi)} \right]; \Psi = \alpha + kd\cos(\theta)$$

$$AF = \left[1 + e^{j(\alpha kd\cos(\theta))} + e^{j(2\alpha + 2kd\cos(\theta))} + \cdots + e^{j((N-1)\alpha + (N-1)kd\cos(\theta))} \right] \quad AF = \sum_{n=1}^{N} e^{j.(n-1).\Psi}$$

$$AF e^{j\Psi} = \sum_{n=1}^{N} e^{jn\Psi}$$

Subtracting these two last equations we will have:

$$AF\left(e^{j\Psi}-1\right)=\left(e^{jN\Psi}-1\right) \text{ ; i.e ; } \quad AF=\frac{\left(e^{jNY}-1\right)}{\left(e^{jY}-1\right)}=\frac{e^{j\frac{N}{2}Y}\left(e^{j\frac{N}{2}Y}-e^{-j\frac{N}{2}Y}\right)}{e^{j\frac{1}{2}Y}\left(e^{j\frac{1}{2}Y}-e^{-j\frac{1}{2}Y}\right)}$$

$$AF=\frac{e^{j\frac{N}{2}\Psi}}{e^{j\frac{1}{2}\Psi}}=e^{j\frac{N-1}{2}\Psi}\frac{\sin\left(\frac{N\Psi}{2}\right)}{\sin\left(\frac{\Psi}{2}\right)}$$

Therefore AF is reduced to the real part because the exponential part can be added to the phases of E_0 in the equation $E_\theta = E_0 AF$.

$$AF=\frac{\sin\left(\frac{N\Psi}{2}\right)}{\sin\left(\frac{\Psi}{2}\right)}$$

The angle made by the lobes verifies the equation AF = 0 i.e. :

$$\sin\left(\frac{N\Psi}{2}\right)=0$$

$$\frac{N\Psi}{2}=\pm n\pi \Rightarrow \alpha + kd\cos\left(\theta\right)=\frac{\pm 2n\pi}{N}$$

$$\theta=\cos^{-1}\left[\frac{1}{kd}\left(-\alpha\pm\frac{2n\pi}{N}\right)\right] \qquad \begin{array}{l} n=1,2,3,... \\ n\neq 0,N,2N,3N,.... \end{array}$$

$$\theta=\cos^{-1}\left[\frac{1}{kd}\left(-\alpha\pm 2m\pi\right)\right] \qquad m=0,1,2,3...$$

$$\Rightarrow \theta=\cos^{-1}\left[\frac{1}{kd}\left(-\alpha\pm 2m\pi\right)\right] \qquad m=0,1,2,3...$$

$$\theta=\cos^{-1}\left[\frac{\lambda}{2\pi d}\left(-\alpha\pm 2m\pi\right)\right]$$

For $m=0$, the angle will be maximum :

$$\theta=\cos^{-1}\left[\frac{\lambda}{2\pi d}\left(\alpha\right)\right]$$

$$\cos\theta=\frac{\lambda\alpha}{2\pi d}$$

Like, $\omega = 2\pi f = 2\pi \dfrac{c}{\lambda} \Rightarrow \dfrac{\lambda}{2\pi} = \dfrac{c}{\omega}$

So, $\cos\theta = \dfrac{c\alpha}{\omega d} \Rightarrow \alpha = \dfrac{\omega d \cos(\theta)}{c}$

- ULA relative to the horizontal

ULA with uniform amplitude and progressive phase deflects its lobe at an upward angle, the uniform phases must follow the equation:

$$\alpha = \frac{\omega d \sin(\theta)}{c} \tag{3}$$

Where, α : the uniform phase, ω : the frequency of modulation, d : the antenna spacing, c : the speed of light; θ : the angle from horizontal and respect the horizontal condition. The angle will be $\theta' = \dfrac{\pi}{2} - \theta$.

By usisng Formula 2,

$$\alpha = \frac{\omega d \cos\theta'}{c} = \frac{\omega d \cos\left(\theta - \dfrac{\pi}{2}\right)}{c} = \frac{\omega d \sin(\theta)}{c}$$

- BeamForming Simple using multi-targeting ULA

For the main lobe of the antenna to move towards a target located at an angle with respect to the horizontal of the radar MIMO emitter, it is necessary to send a signal on M antennas spaced respectively by distance d:

$$\begin{cases} x_1(t) = s \\ x_2(t) = se^{-j\alpha} \\ x_3(t) = se^{-j.2.\alpha} \\ \quad\vdots \\ x_M(t) = se^{-j.(M-1).\alpha} \end{cases} \Rightarrow \alpha = \frac{\omega d \sin(\theta)}{c} \tag{4}$$

ULA with uniform amplitude and progressive phase deflects its lobe at an upward angle; the uniform phases must follow the equation:

$$\alpha = \frac{\omega d \sin(\theta)}{c}$$

An equation with a uniform phase and progressive amplitude has the form :

$$x_T(t) = se^{-j.(T-1).\alpha}$$

- BeamForming Multi-targeting MIMO ULA

To direct the antenna's main lobe to multiple targets, located at an angle to the horizontal of the base station. Each target wants to send a signal $s_i(t)$ using M antennas spaced respectively by the distance d :

$$
\begin{cases}
x_1(t) = \sum_{i=1}^{n} s_i \\[2mm]
x_2(t) = \sum_{i=1}^{n} s_i e^{-j\alpha_i} \\[2mm]
x_3(t) = \sum_{i=1}^{n} s_i e^{-j.2.\alpha_i} \qquad \Rightarrow \alpha_i = \dfrac{\omega d \sin(\theta_i)}{c} \\[2mm]
\quad\vdots \\[2mm]
x_M(t) = \sum_{i=1}^{n} s_i e^{-j.(M-1).\alpha_i}
\end{cases}
$$

Each signal will be send by a carrier; by :

$$
x_T(t) = \sum_{i=1}^{n} s_i e^{-j.(T-1).\alpha_i}
\tag{6}
$$

Because the antennas are uniform in amplitude and progressive in phase :

$$
\Rightarrow \alpha_i = \frac{\omega d \sin(\theta_i)}{c}
$$

2.2. Phased Array Antenna using Uniform Rectangular Antenna (URA)

• Theory on URA antennas

By using N-antennas along the abscissa axes and M-antennas along the ordinate axes, to rotate the antenna propagation lobes according to a polar coordinate of angles; The uniform phase has the equation:
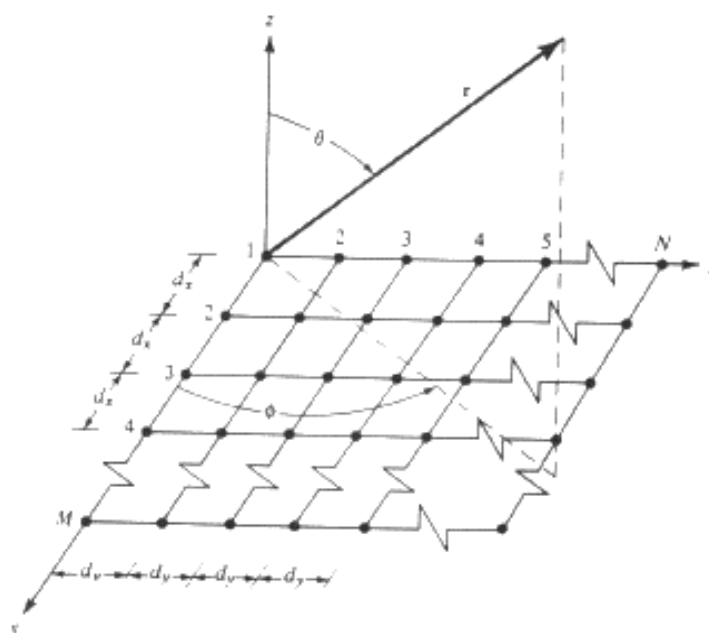
Fig -3: Representation of Uniform Rectangular Antenna

$$\alpha_{ij} = (i-1)\beta_x + (j-1)\beta_y, \quad \forall i = \{1,\cdots,N\}, \quad \forall j = \{1,\cdots,M\}$$

$$\beta_x = -\frac{\omega}{c}d_x \sin\theta\cos\phi$$

$$\beta_y = -\frac{\omega}{c}d_y \sin\theta\sin\phi$$

$$AF_{x1} = \sum_{m=1}^{M} I_{m1} e^{j(m-1)\left(kd\sin(\theta)\cos(\phi)+\beta_x\right)}$$

(7)

With,

$\sin(\theta)\cos(\phi) = \cos(\gamma_x)$: The direction along the abscissa axis

d_x : The space between the antennas along the x-axis ; β_x : The progressive phase along the abscissa axis

I_{m1} : The amplitude of excitation at coordinates $x = (m-1)d_x$, $y = 0$

d_y : The space between the antennas along the ordinate axes ; β_y : The progressive phase along the ordinate axis

I_{1n} : The amplitude excitation at coordinates $x = 0$, $y = (n-1)d_y$

$$AF_{x1} = \sum_{m=1}^{N} I_{m1} e^{j(m-1)(kd_x \sin\theta\cos\phi+\beta_x)}$$

$$AF_{1y} = \sum_{n=1}^{N} I_{1n} e^{j(n-1)(kd_y \sin\theta\sin\phi+\beta_y)}$$

$$AF = AF_{x1} * AF_{1y}$$

$$AF = \sum_{n=1}^{N} I_{1n} \left[\sum_{m=1}^{M} I_{m1} e^{j(m-1)(kd_x \sin\theta\cos\phi+\beta_x)} \right] e^{j(n-1)(kd_y \sin\theta\sin\phi+\beta_y)}$$

Since the amplitudes are uniform then :

$$\forall m \in [1;M]; n \in [1;N] \Rightarrow I_{mn} = I_0$$

$$AF = I_0 \sum_{n=1}^{N} \left[\sum_{m=1}^{N} I_{m1} e^{j(m-1)(kd_x \sin\theta\cos\phi+\beta_x)} \right] e^{j(n-1)(kd_y \sin\theta\sin\phi+\beta_y)}$$

Like in ULA,

$$AF = I_0 \left\{ \frac{1}{M} \frac{\sin\left(M\frac{\psi_x}{2}\right)}{\sin\left(\frac{\psi_x}{2}\right)} \right\} \left\{ \frac{1}{N} \frac{\sin\left(N\frac{\psi_y}{2}\right)}{\sin\left(\frac{\psi_y}{2}\right)} \right\}$$

Where,

$$\begin{cases} \psi_x = k\sin\theta\cos\phi + \beta_x \\ \psi_y = k\sin\theta\sin\phi + \beta_y \end{cases}$$

The lobes therefore have the equation:

$$\begin{cases} S_{x_M} = \dfrac{1}{M} \dfrac{\sin\left(M\frac{\psi_x}{2}\right)}{\sin\left(\frac{\psi_x}{2}\right)} \\[4ex] S_{y_N} = \dfrac{1}{N} \dfrac{\sin\left(N\frac{\psi_y}{2}\right)}{\sin\left(\frac{\psi_y}{2}\right)} \end{cases} \tag{8}$$

And its lobes are located in the following angles:

$$\begin{cases} kd_x \sin\theta_m \cos\phi_m + \beta_x = \pm 2\pi m, & m = 0,1,\cdots \\ kd_y \sin\theta_m \sin\phi_m + \beta_y = \pm 2\pi m, & n = 0,1,\cdots \end{cases}$$

So, using azimuth and elevation with polar coordinates

$$\begin{cases} \beta_x = -\dfrac{\omega}{c} d_x \cos\varphi\cos\phi \\[3ex] \beta_y = -\dfrac{\omega}{c} d_y \cos\varphi\sin\phi \end{cases}$$

Where,

ϕ : The azimuth ; $\theta = \dfrac{\pi}{2} - \varphi$: The complement of elevation

- BeamForming Multi-target MIMO URA

The transmitter wants directing the antenna's main lobe to multiple targets located to azimuth ϕ_i and elevation φ_i .

Each targets want to send signal $s_k(t)$ in the planar antenna spaced resp. by d_x and d_y :

$$X_{x,y}(t) = \sum_{i=1}^{n} s_i e^{-j.(M-1).\alpha_i [x,y]} \tag{9}$$

$$\Rightarrow \begin{cases} \forall x = \{1, \cdots, N\}, \quad \forall y = \{1, \cdots, M\} \\ \alpha_i[x, y] = (x-1)\beta_x + (y-1)\beta_y, \\ \beta_x = -\dfrac{\omega}{c} d_x \cos|\varphi_S - \varphi_i| \cos|\phi_S - \phi_i| \\ \beta_y = -\dfrac{\omega}{c} d_y \cos|\varphi_S - \varphi_i| \sin|\phi_S - \phi_i| \end{cases} \tag{10}$$

2.3. FMCW with MIMO ULA

- Models of FMCW with MIMO ULA

In this section, we address the system model and data structure considered in this paper. We consider the FMCW radar system, which has one transmitted (TX) antenna and K received (RX) antennas, as shown in Figure 4.
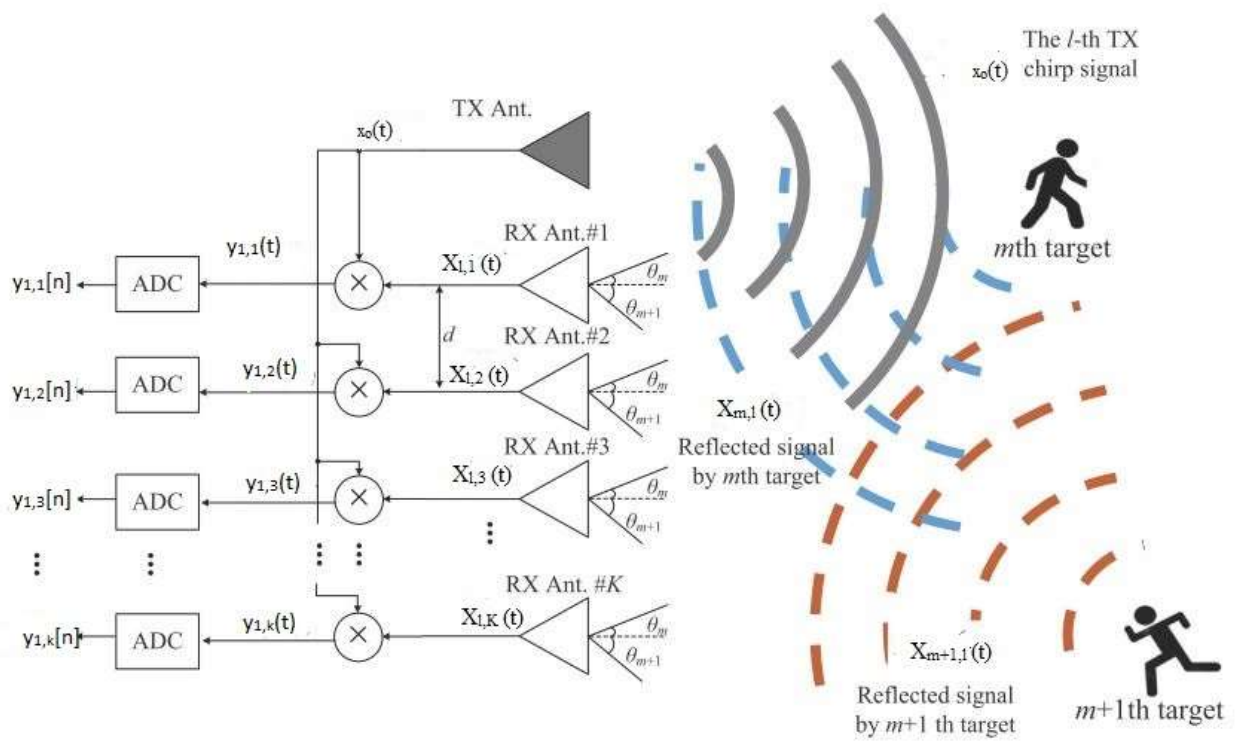
Fig -4: System model of the considered FMCW radar (1 TX and K RX antennas)

This section discusses the different models of FMCW radar systems and the notations used in them. We considerreflected signals of FMCW radar in order to detect the ranges, the velocities, and the azimuth distributions of targets. To facilitate an easier understanding of the concepts, we initially consider the case of a single target, after which we extend this to the case of multiple targets. Consider a uniform linear array (ULA) of *K* receiving (RX) antenna arrays with distance *d* between adjacent arrays and a single transmitted (TX) antenna. The TX FMCW signal denoted by $x_0(t)$ is shown in Figure 5 (a) and is expressed as :

$$x_o(t) = \exp\left(j2\pi\left(f_0 t + \frac{\mu t^2}{2}\right)\right) \tag{11}$$

Where $0 \le t \le T$, f_0 is the frequency modulation period during which the TX frequency sweeps over the entire bandwidth B, and μ is the chirp rate, i.e., $\mu = B/T$. All *L* chirp signals are transmitted during a frame; i.e., $T_F = TL$.

The signal reflected from the target is received with delay τ and Direction of Arrival (DOA) θ at the k-th array, as shown in Figure 6. Here, the l-th chirp slot is denoted by $x_{l,k}(t)$ and is expressed as :

$$x_{l,k}(t) = a_o x_o(t - \tau) exp(j2\pi f_D \, lT) \times exp(j.2\pi.d.k.\sin(\theta)/\lambda) + \tilde{w}_{l,k}(t)$$

(12)

Where, a_o is the complex amplitude, $\tilde{w}_{l,k}(t)$ is the additive white Gaussian noise (AWGN) signal, fD is the Doppler frequency due to the moving of the target and λ is the wavelength. By denoting the velocity term as $v^l(f_D) = exp(j2\pi f_D \, lT)$ and the DOA term as $\psi^k(\theta) \, exp(j.2\pi.d.k.\sin(\theta)/\lambda) + ;$ $x_{l,k}(t)$ can simply be represented as follows :

$$x_{l,k}(t) = a_o x_o(t - \tau) v^l(f_D)\psi^k(\theta) + \tilde{w}_{l,k}(t)$$

(13)

The beat signal $y_k(t)$ is expressed by omitting θ and fD for simplicity, as follows

$$y_{l,k}(t) = x_{l,k}(t) \times x^*_o(t) = a \, exp(-j.2\pi.f_b.t).v^l.\psi^k + w_{l,k}(t)$$

$$y_{l,k}(t) = ax_b(t).v^l.\psi^k + w_{l,k}(t)$$

(14)

where $f_b = \mu\tau$ is the beat frequency and $xb(t)$ is the sinusoid term in the beat signal. In addition, a and $wl,k(t)$ are expressed as follows:

$$a = a_0 exp\left(-j2\pi(f_0\tau - \mu\tau^2/2)\right)$$

(15)

$$w_{l,k} = \tilde{w}_{l,k}(t).x^*_o(t)$$

(16)

An analog-to-digital conversion (ADC) of $y_{l,k}(t)$, the discrete time model of (14) with the sampling frequency $f_s = \dfrac{1}{T_s}$ is denoted by $y_{l,k}[n] = y_{l,k}(n.T_s)$ for $n = 0,1,\dots,N_s - 1$ where T_s is the sampling time interval and $N_s = \dfrac{T}{T_s}$ and $y_{l,k}[n]$ can be expressed as follows :

$$y_{l,k}[n] = a.x_b[n.T_s]v^l\psi^k + w_{l,k}[n]$$

(17)

- Conventional 3D-FFT detection algorithm for surveillance applications

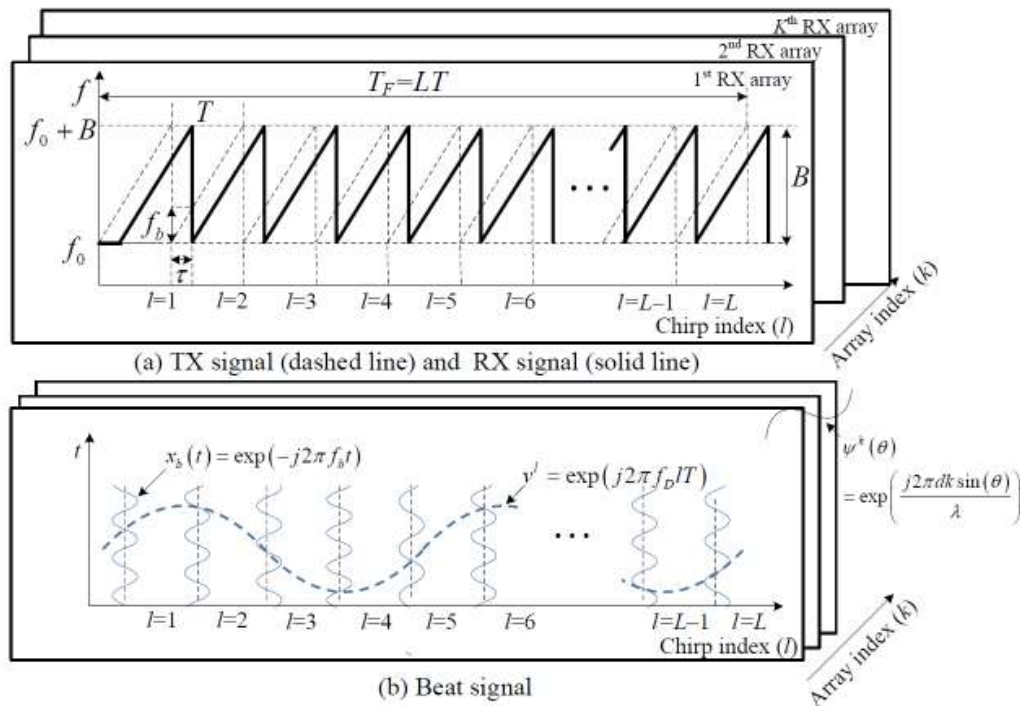(a) TX signal (dashed line) and RX signal (solid line)
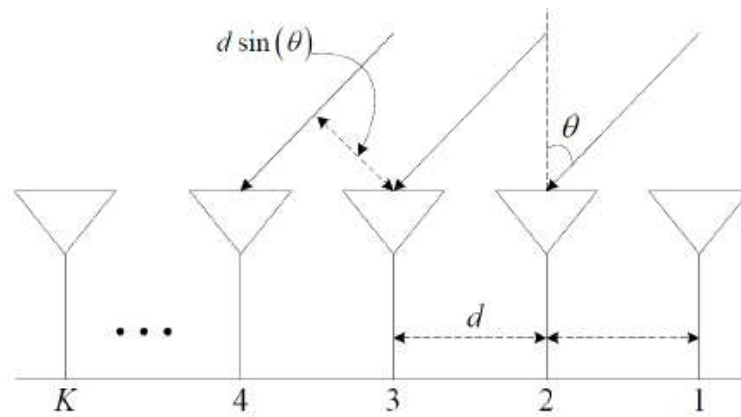
(b) Beat signal

Fig -5: Waveforms of FMCW radar

Fig -6: DOA modeling

This section introduces the conventional detection algorithm using the 3D-FFT. In order to estimate the range, the velocity and the angle of a target, a data cube composed of the 3D beat signal in (17) is employed. The conventional algorithm performs 3D-FFT operations on the data cube in the time (range) domain, the ramp (chirp) domain, and the array domain.
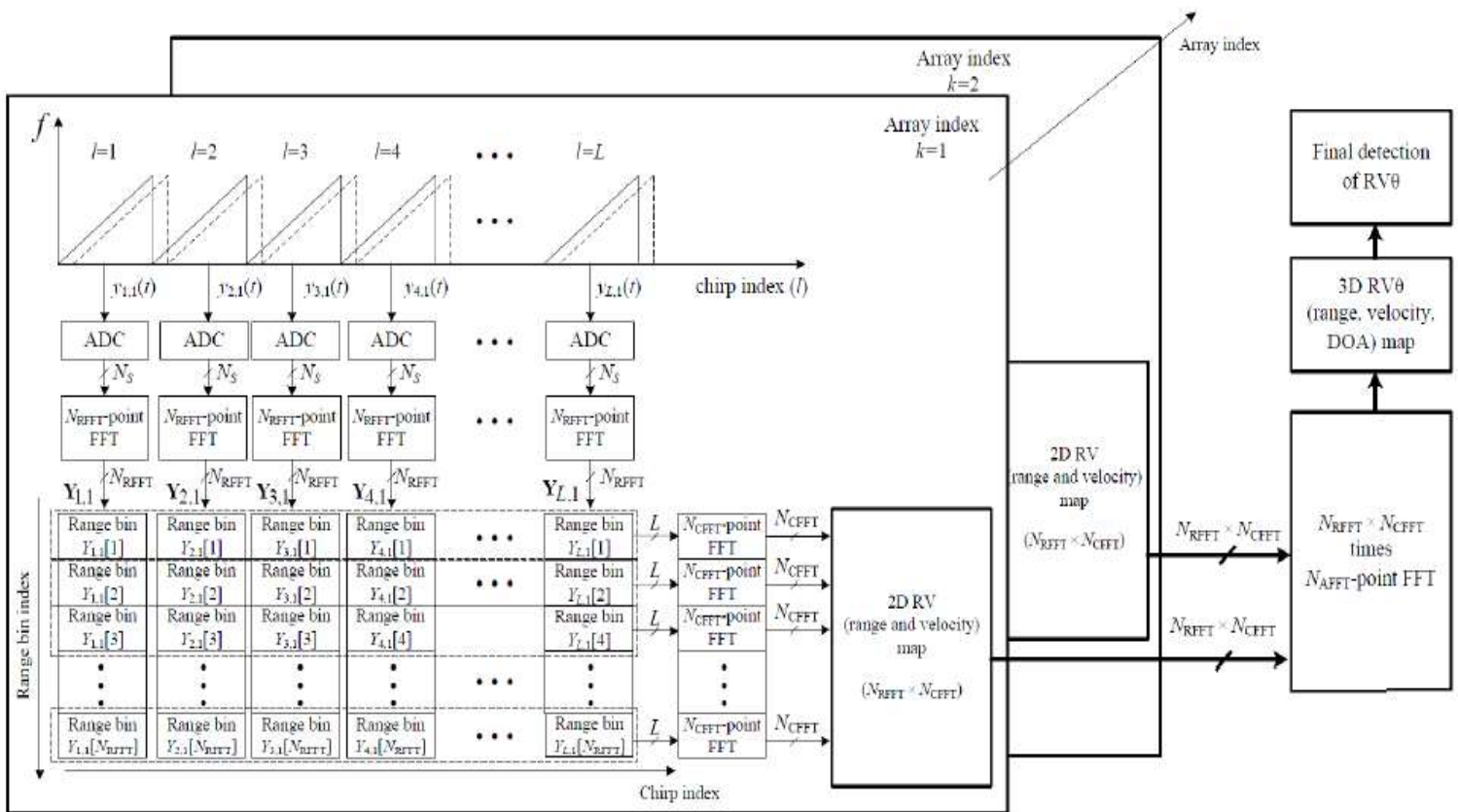

Fig -7: 3D-FFT for DOA estimation with ULA RADAR MIMO receiver

First, as shown in Figure 7, a N_{RFT}-point FFT operation on the data cube in the time (range) domain is performed, where N_{RFT} denotes the number of points of the FFT in the range domain :

$$Y_{l,k}[u] = \sum_{n=0}^{N_s-1} y_{l,k}[n].W_{N_{RFT}}^{qn} \tag{18}$$

Where $0 \le u \le N_{RFT} - 1$; W_N is the N-point DFT opération i.e $W = ex(-j2\pi/N)$.

That is, the range domain N_{RFFT}-point FFT output vector at the l-th chirp and k-th array $Y_{l,k} = \left[Y_{l,k}[1], Y_{l,k}[2], \dots . Y_{l,k}[N_{RFFT}]\right]$ is obtained. Subsequently, the N_{CFFT} point FFT operation on $Y_{l,k}$ in the chirp domain is conducted where N_{CFFT} is the number of points for the FFT in the chirp domain. This gives the range and velocity map with $N_{RFFT} \times N_{CFFT}$. Finally, with an N_{AFFT} -point FFT operation on the range and velocity map with $N_{RFFT} \times N_{CFFT}$ in the array domain, the 3D map which reflects the range, velocity and DOA is obtained.

However, in order to perform a 3D FFT, very high complexity is required, as is well known. This causes the processing time and cost to increase.

Meanwhile, in order to reduce the computational complexity of multi-dimensional FFT operations, FFT algorithms with reduced dimensions have been proposed.

In these algorithms, the range of the FFT output is initially determined, after which the peak of the magnitude of the FFT output is detected. The authors use the characteristic by which the targets exist only in the range bin with the peak of the magnitude of the FFT output. They conduct a chirp-domain FFT operation on only the range bins in which the target exists. By not performing the chirp-domain FFT on the range bins without a target, they reduce the computational complexity of the multi-dimensional FFT operation.

However, these algorithms require additional algorithms such as clutter mitigation or moving target indicator algorithms because they do not distinguish between clutter and the target.

- Resolution estimation with MIMO ULA receivere with FMCW RADAR

n the surveillance radar systems, the first important issue is a quick determination of the presence of the targets of interest. In cases where there are no targets of interest, we do not need to use resources unnecessarily. That is, the detection algorithm should be run only if there is a target of interest. To this end, the proposed method initially determines whether or not a target exists. Parameter detection operations are performed after it is determined that a target exists.

Figure 7 illustrates the structure of the proposed algorithm. As shown in Figure 8, the proposed algorithm properly selects the range and velocity map with $N_{RFFT} \times N_{CFFT}$. Finally, with an N_{AFFT} -point FFT operation on the range and velocity map with $N_{RFFT} \times N_{CFFT}$ in the array domain, the 3D map which reflects the range, velocity and DOA is obtained. However, in order to perform a 3D FFT, very high complexity is required, as is well known. This causes the processing time and cost to increase.

Two beat signals among all L beat signals according to the velocity of interesting target; that is, the p-th and the q-th beat signals, $y_{p,k}[n]$ and $y_{q,k}[n]$, are selected. We then subtract the two signals, with this action denoted by $d_{pq,k}[n]$, as follows

$$d_{pq,k}[n] = y_{p,k}[n] - y_{q,k}[n] = ax_b[nt_s]\Psi^k(v^p - v^q) + w_{p,k}[n] - w_{q,k}[n] \qquad (19)$$

Generally, clutter or stationary targets do not move. Accordingly, the Doppler effect does not occur. On the other hand, when the target moves, the Doppler effect arises, and the phase changes as the index of the chirp increases. If there is no moving target, the Doppler frequency equals zero; i.e., $f_D = 0$. Therefore, only the noise terms remains in (19) because $v^p(0) = v^q(0)$. This implies that only the noise term is input as the N_{RFFT}-point FFT input. On the other hand, if there is a moving target, vp and vq are not equal except when $p = q$ and $q = p + iT$, where i is the integer number and T is the chirp duration..
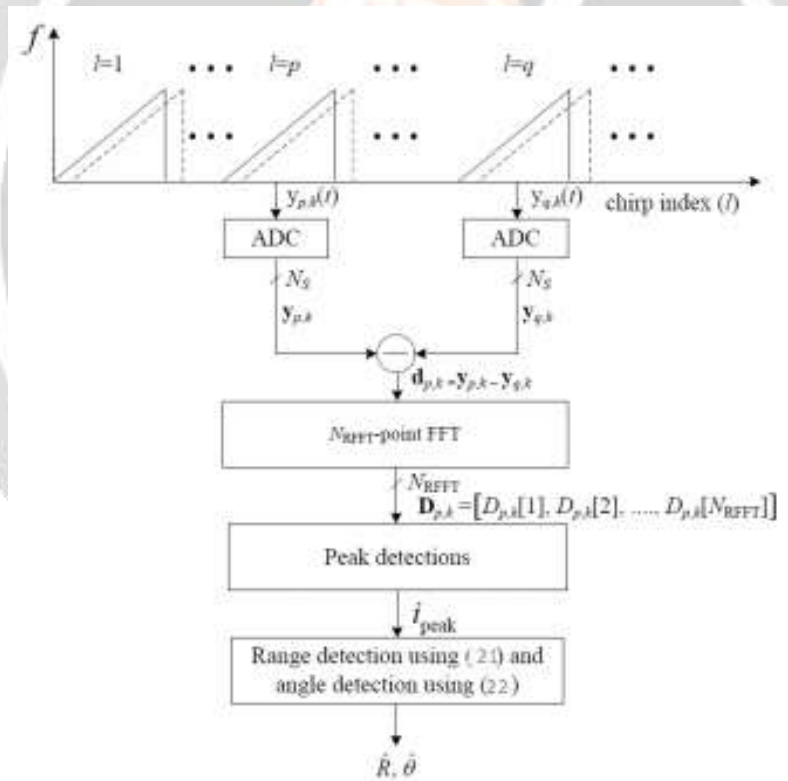

Fig -8: 3D-FFT for DOA estimation with ULA RADAR MIMO receiver

Therefore, for simplicity, by omitting the noise terms, (18) is simply expressed as :

$$d_{pq,k}[n] = ax_b[nt_s]\Psi^k \qquad (20)$$

Where $\alpha = a(v^p - v^q)$. From (20), it can be seen that the beat signal $x_b[nt_s]$ including the range information and the DOA term Ψ^k still exists.

Here, we properly select two chirps, i.e., p and q. This is done because we want to avoid a case in which the proposed algorithm does not work properly. For example, if the phase changes at the two chirps are symmetrical, the output after subtraction may be zero, as if there is no moving target. However, the duration of one frame is relatively short compared to the moving time of the target. By properly selecting two chirps, we can avoid cases in which the phase changes of two chirps are symmetrical.

In order to estimate the range of the target, we perform FFT on $d_{pq,k}[n]$ with respect to the sample domain n, as in (18); thus, the N_{RFFT}-FFT output of $d_{pq,k}[n]$ denoted by $d_{pq,k}[u]$ is obtained. We then obtain the index i_{peak} corresponding to the beat frequency of $d_{pq,k}[n]$ through the peak detection of $|d_{pq,k}[u]|$ for $0 \leq u \leq N_{RFFT} - 1$. Figure 9 shows an example of the result of the peak detection of $d_{pq,k}[u]$ when $i_{peak} = 35$. From the obtained peak i , the estimated range $\hat{R}$ is calculated as :

$$\hat{R} = \frac{c \times \hat{t}}{2} = \frac{c \times \hat{f}_b}{2\mu} = \frac{c \times i_{peak} \times f_s}{2\mu N_{RFFT}}$$

(21)

where c is the speed of light, $\hat{t}$ is the estimated delay, and $\hat{f}_b$ is the estimated beat frequency.
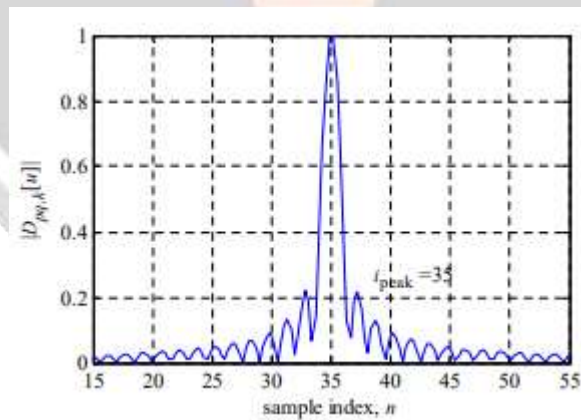

Fig -9 : Example of the result of peak detection of $|d_{pq,k}[u]|$

Furthermore, we use only two RX antennas in order to ensure a low cost and low complexity. The proposed algorithm does not perform array-domain FFT in order to detect the DOA information. In the proposed algorithm, the DOA is estimated using the phase change between two arrays instead of an array-domain FFT, as follows :

$$\hat{\theta} = sin^{-1}\left[\angle\left(Y_{p,1}^{*}[i_{peak}]Y_{p,2}[i_{peak}]\right)\right] = sin^{-1}\left[\angle\left(\beta exp\left(j2\pi dsin(\theta)/\lambda\right)\right)\right]$$

(22)

where β denotes the term apart from except DOA term in (13). Of course, this simple DOA estimation is only possible in the condition with a single target. However, even with multiple targets, if the ranges or velocities of the targets are not identical, the outcome will be similar to that of a single-target condition in a FMCW radar system.

2.4. FMCW with MIMO URA

- System

As shown in Figure 10, an $M \times N$ dimensional uniform rectangular array is placed on the $X - Y$ plane, where M and N represent the number of antenna elements arranged in the X-axis and Y-axis directions of the array, and the inter-element spacing is $\lambda/2$, where λ is the wavelength of the source signals. Assume K far-field sources from $\theta = (\theta_1, \theta_2, ..., \theta_k)$, $\emptyset = (\emptyset_1, \emptyset_2, ..., \emptyset_k)$ impinge on the array.
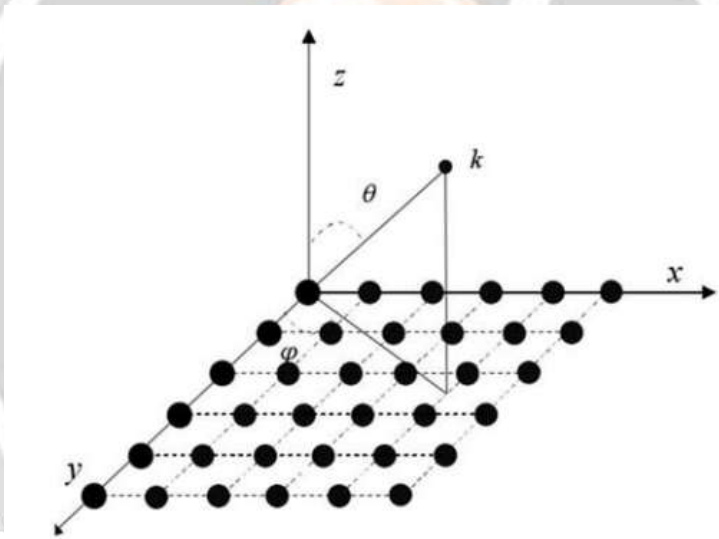
Fig -10 : Uniform rectangular array

Let the element of the coordinate origin be the reference element, and the single snapshot data received by the array can be expressed as :

$$X = AS + N$$

(23)

Where $A = [a(\theta_1, \emptyset_1), ..., a(\theta_k, \emptyset_k)] \in \mathbb{C}^{MN \times K}$ is the steering matrix with $a(\theta_k, \emptyset_k) = a_x(\theta_k, \emptyset_k) \otimes a_y(\theta_k, \emptyset_k)$,

where $\quad a_x(\theta_k, \emptyset_k) = [1, e^{-j2\pi d \sin\theta_k \cos\emptyset_k/\lambda}, \dots, e^{-j2\pi (M-1)d \sin\theta_k \cos\emptyset_k/\lambda}]^r \in \mathbb{C}^{M \times K}$ $\quad$ and

$a_x(\theta_k, \emptyset_k) = [1, e^{-j2\pi d \sin\theta_k \cos\emptyset_k/\lambda}, \dots, e^{-j2\pi (N-1)d \sin\theta_k \cos\emptyset_k/\lambda}]^r \in \mathbb{C}^{N \times K}$,

$S = [S_1, \dots, S_k]^r \in \mathbb{C}^{K \times 1}$ is the narrow-band noncircular signal vector, $N = [n_1, \dots, n_{MN}]^r \in \mathbb{C}^{MN \times 1}$

denotes the additive white Gaussian noise and $E[NN^H] = \sigma^2 I_{MN}$.

- DOA Estimation Algorithm

Discrete Fourier transform (DFT) has been applied to DOA estimation for a long time, and the DOA estimation algorithm based on DFT is considered as a non-parametric spectrum analysis algorithm. Since the optimal resolution of this algorithm is inversely proportional to the number of antennas M, it performs worse than some parameterized subspace algorithms for traditional small array and is gradually substituted by the latter algorithms. Correspondingly, the DFT-based DOA estimation algorithms were rarely studied in the literature of the last decade. However, DFT algorithms have their advantages in large-scale arrays since the resolution of DFT algorithms can be significantly improved with the very large number of antennas.

- The Initial Estimation Based on 2D-DFT

The normalized 2D-DFT of the received data matrix can be given by $\tilde{F}_k = F_M X_{MN} F_N$, where X_{MN} is the $M \times N$ received data matrix. The (p, q) -th element of X_{MN} is represented by $x_{(p-1)N+q}(t)$. F_M and F_N are normalized DFT matrices, and the (p, q) -th element can be given by $[F_M]_{pq} = e^{-j\frac{2\pi}{M}pq}/\sqrt{M}$ and $[F_N]_{pq} = e^{-j\frac{2\pi}{N}pq}/\sqrt{N}$, respectively. Considering no noise interference and the number of antennas tends to infinity, i.e., M N, $\to \infty$, we can obtain that $\frac{M}{2}\sin\theta_k \cos\emptyset_k$ and $\frac{N}{2}\sin\theta_k \cos\emptyset_k$ are both integers, and all energy is concentrated at the point $(\frac{M}{2}\sin\theta_k \cos\emptyset_k, \frac{N}{2}\sin\theta_k \cos\emptyset_k)$, as shown in Figure 11. The DOA estimation angle can be uniquely determined by searching this non-zero point.

However, the number of antennas in practical scenarios is limited, then $\frac{M}{2}\sin\theta_k \cos\emptyset_k$ and $\frac{N}{2}\sin\theta_k \cos\emptyset_k$, are not integers. As a result, the energy of $\tilde{F}_k$ will leak to the adjacent points of $\left(\left[\frac{M}{2}\sin\theta_k \cos\emptyset_k\right], \left[\frac{N}{2}\sin\theta_k \cos\emptyset_k\right]\right)$, as shown in Figure 12. In fact, $\tilde{F}_k$ consists of sinc functions, and the amount of leaked energy is inversely proportional to M, N while proportional to $\left|\frac{M}{2}\sin\theta_k \cos\emptyset_k - \left[\frac{M}{2}\sin\theta_k \cos\emptyset_k\right]\right|$ and $\left|\frac{N}{2}\sin\theta_k \cos\emptyset_k - \left[\frac{N}{2}\sin\theta_k \cos\emptyset_k\right]\right|$. For large-scale URA arrays, M, $N \gg 1$, most energy of $\tilde{F}_k$ is still concentrated at the point $\left(\left[\frac{M}{2}\sin\theta_k \cos\emptyset_k\right], \left[\frac{N}{2}\sin\theta_k \cos\emptyset_k\right]\right)$ and its around, and the initial DOA value can be estimated using the peak position of $\tilde{F}_k$.
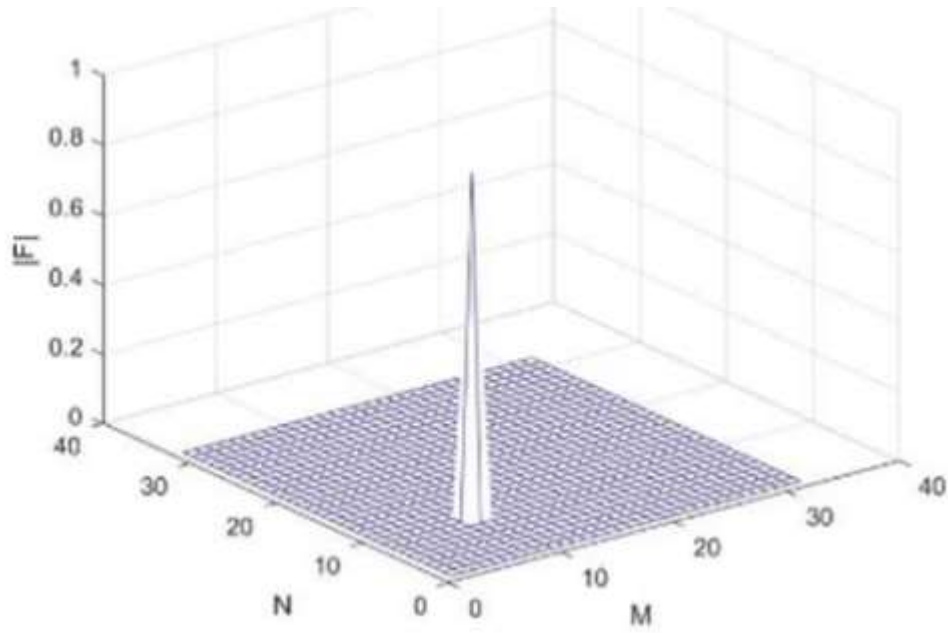
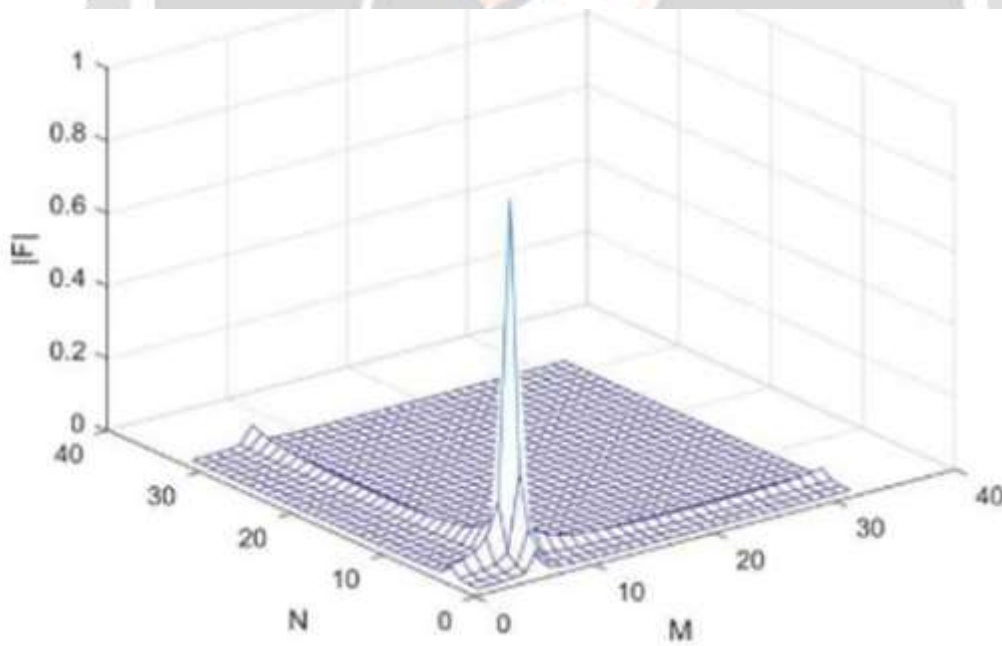**Fig -11 :** The case without energy leakage for large-scale URA

Fig -12 : The case with energy leakage for large-scale URA

The peak position of the k-th source is expressed as (m_k, n_k). Assume that the impact of leaks is neglected, then
$\frac{M}{2} sin\theta_k cos\emptyset_k = m_k, \frac{N}{2} sin\theta_k cos\emptyset_k = n_k$, the DOA value of the k-th source is given by :

$$\begin{cases} \theta_k = arcsin(u_k^2 + v_k^2) \\ \emptyset_k = arctan\left(\frac{v_k}{u_k}\right) \end{cases}$$

(24)

Where $u_k = \frac{\lambda m_k}{Md}$ and $v_k = \frac{\lambda n_k}{Nd}$

- The Precise Estimation Based on Phase Rotation

The phase rotation factors with respect to α and β are respectively defined as

$$\begin{cases} \Phi_M(\Delta\alpha_k) = diag(1, e^{j\Delta\alpha_k}, \dots, e^{j(M-1)\Delta\alpha_k}) \\ \Phi_N(\Delta\beta_k) = diag(1, e^{j\Delta\beta_k}, \dots, e^{j(M-1)\Delta\beta_k}) \end{cases}$$

(25)

Where $\Delta\alpha_k \in \left[-\frac{\pi}{M}, \frac{\pi}{M}\right]$ and $\Delta\beta_k \in \left[-\frac{\pi}{N}, \frac{\pi}{N}\right]$. The phase rotation operation can be given by
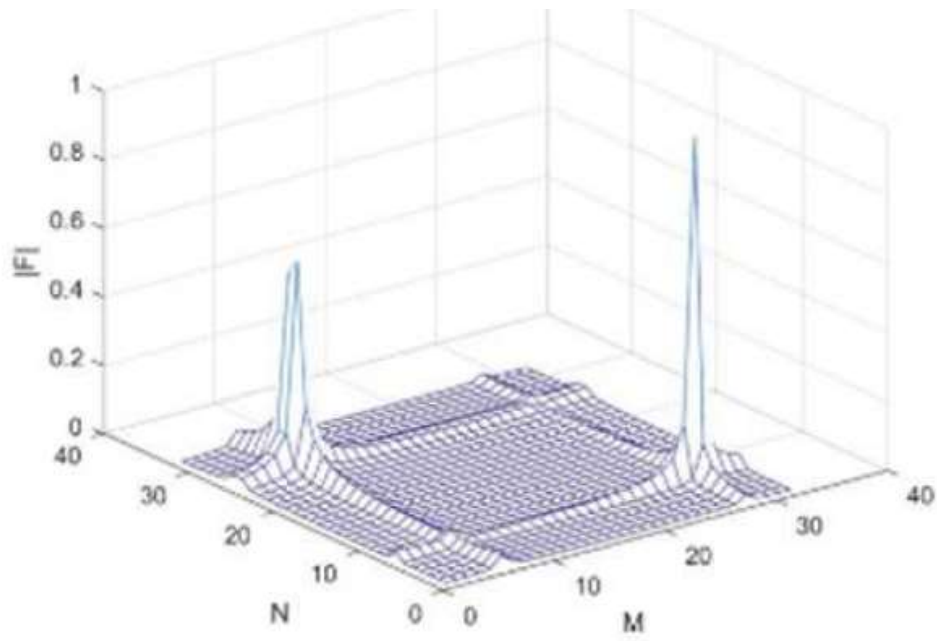
$$\tilde{F}_k^{ro} = F_M \Phi_M(\Delta\alpha_k) X_{MN} \Phi_N(\Delta\beta_k) F_N$$

(26)

When $\Delta\alpha_k = (\frac{2\pi m_k}{M} - \frac{2\pi d}{\lambda} sin\theta_k cos\emptyset_k) \in \left[-\frac{\pi}{M}, \frac{\pi}{M}\right]$
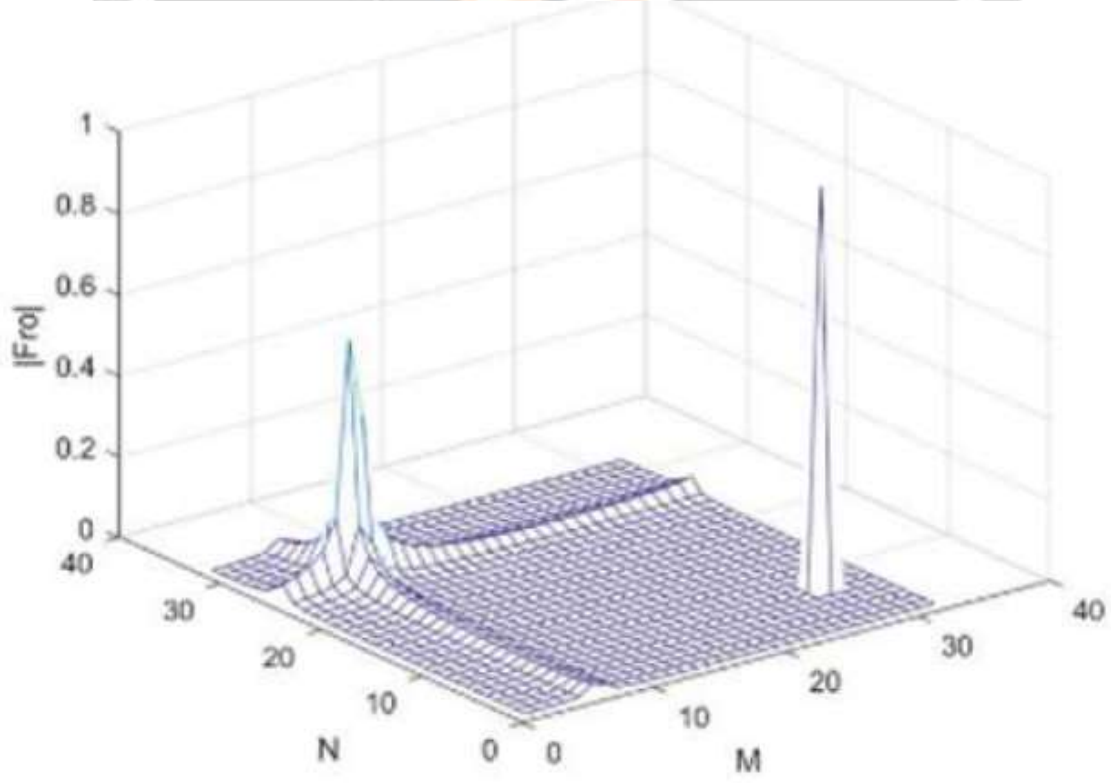
and $\Delta\beta_k = (\frac{2\pi n_k}{N} - \frac{2\pi d}{\lambda} sin\theta_k cos\emptyset_k) \in \left[-\frac{\pi}{N}, \frac{\pi}{N}\right]$, $\tilde{F}_k^{ro}$ only has one non-zero point, and the sum of $\Delta\alpha_k$ and $\Delta\beta_k$ is called the optimal phase shift amount.

$u_k' = u_k - \frac{\Delta\alpha_k}{2\pi d}$, $v_k' = v_k - \frac{\Delta\beta_k}{2\pi d}$. At this time, the precise DOA estimate of the first source is given by

$$\theta_k = arcsin(u_k^2 + v_k^2) = arcsin\left(\left(\frac{\lambda m_k}{Md} - \frac{\Delta\alpha_k}{2\pi d}\right)^2\right) + \left(\left(\frac{\lambda n_k}{Nd} - \frac{\Delta\beta_k}{2\pi d}\right)^2\right)$$

$$\emptyset_k = arctan\left(\frac{v_k'}{u_k'}\right) = arctan\left(\frac{\frac{\lambda n_k}{Nd} - \frac{\Delta\beta_k}{2\pi d}}{\frac{\lambda m_k}{Md} - \frac{\Delta\alpha_k}{2\pi d}}\right)$$

(27)

Fig -13 : The case without phase rotation

Fig -14: The case with phase rotation for the source ($\theta_1 = -30°, \emptyset_1 = 50°$)

The compression the spectral peaks with phase rotation for the incidences of two far-field narrowband independent sources are shown in Figure 13 and Figure 15, where noise is not considered for better demonstration. The angles of the two incident sources are assumed to be (-30° ,50°) and (-35° , -55°) , respectively.

The optimal phase shift of sources is usually different from each other, as shown in Figure 13 and Figure 15. Hence, it is necessary to find the optimal phase shifts separately.
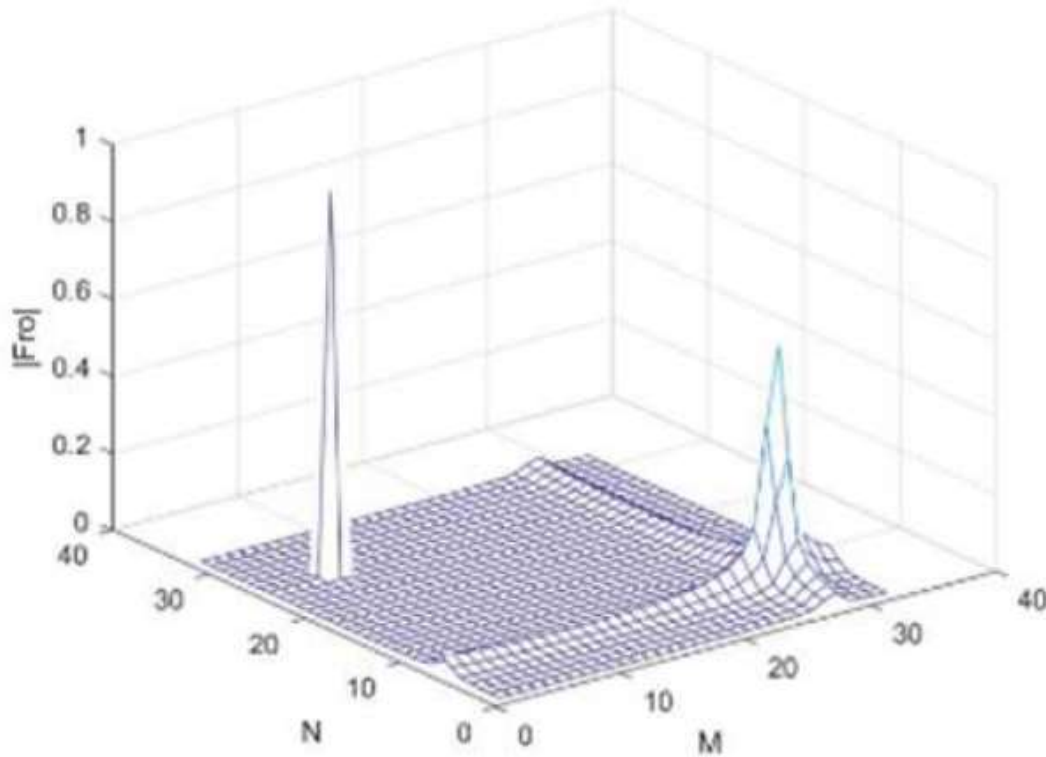

Fig -15: The case with phase rotation for the source ($\theta_2 = -35°, \emptyset_2 = -55°$)

When searching for the best phase shift amount, we can search $\Delta\alpha_k$ in a small area $\left[-\dfrac{\pi}{M}, \dfrac{\pi}{M}\right]$, and similarly search $\Delta\beta_k$ in $\left[-\dfrac{\pi}{N}, \dfrac{\pi}{N}\right]$. The $\Delta\alpha_k$ and $\Delta\beta_k$ which shrink the $k-th$ peak to a point are the optimal phase shift of the $k-th$ source, which can be calculated by

$$\Delta\alpha_k = \arg \max_{\Delta\alpha_k \in \left[-\frac{\pi}{M}, \frac{\pi}{M}\right]} ||F_M(m_k,)\Phi_M(\Delta\alpha_k)X_{MN}F_N(,n_k)||^2$$

$$\Delta\beta_k = \arg \max_{\Delta\beta_k \in \left[-\frac{\pi}{N}, \frac{\pi}{N}\right]} ||F_M(m_k,)X_{MN}\Phi_N(\Delta\beta_k)F_N(,n_k)||^2$$

(28)

Where, the m_k –th row of F_M is giving by $F_M\left(m_k,\right)$ and the n_k –th column of F_N is given by $F_N\left(,n_k\right)$.

- The Implementation Steps of the Proposed Algorithm

Based on the analysis above, the steps of the proposed DOA estimation algorithm in this paper are listed as follows:

1) Perform 2D-DFT transformation on the received data matrix X_{MN} to obtain $\tilde{F}_k$;

2) Calculate the modulus of each element of $\tilde{F}_k$ and search the peak coordinate $\left(m_k, n_k\right)$ of $\tilde{F}_k$;

3) calculate u_k and v_k according to $u_k = \frac{\lambda . m_k}{Md}$ and $v_k = \frac{\lambda . n_k}{Nd}$;

4) search the optimal phase shift $\Delta\alpha_k$ and $\Delta\beta_k$ of the k-th source by utilizing equation (28);

5) calculate u'_k and v'_k according to $u'_k = u_k - \frac{\Delta\alpha_k}{2\pi d}$ and $v'_k = v_k - \frac{\Delta\beta_k}{2\pi d}$;

6) calculate the estimated DOA by utilizing equation (27).

For calculating range, as same formula as the ULA FMCW :

$$\hat{R} = \frac{c \times \hat{t}}{2} = \frac{c \times \hat{f}_b}{2\mu} = \frac{c \times \sqrt{n_k^2 + m_k^2} \times f_s}{2\mu N_{RFFT}}$$

(28)

2. Result and discussion

In Fig-16, we can see the Direction of Arrival of the target of the MIMO Radar receiver using FMCW. This figure presents all angulars represented in the 3D forms and has azimuth and elevation noted on all theories respectively by Φ and θ.

In this simulation, the transmitter sends a specific signal defined in the equation (11) and receiver obtained the same signal as delayed on the multiple antenna receivers. By applying estimation using multiple DFT and URA formula, we can estimate the two angles of the target. This simulation uses three targets, to be estimated.
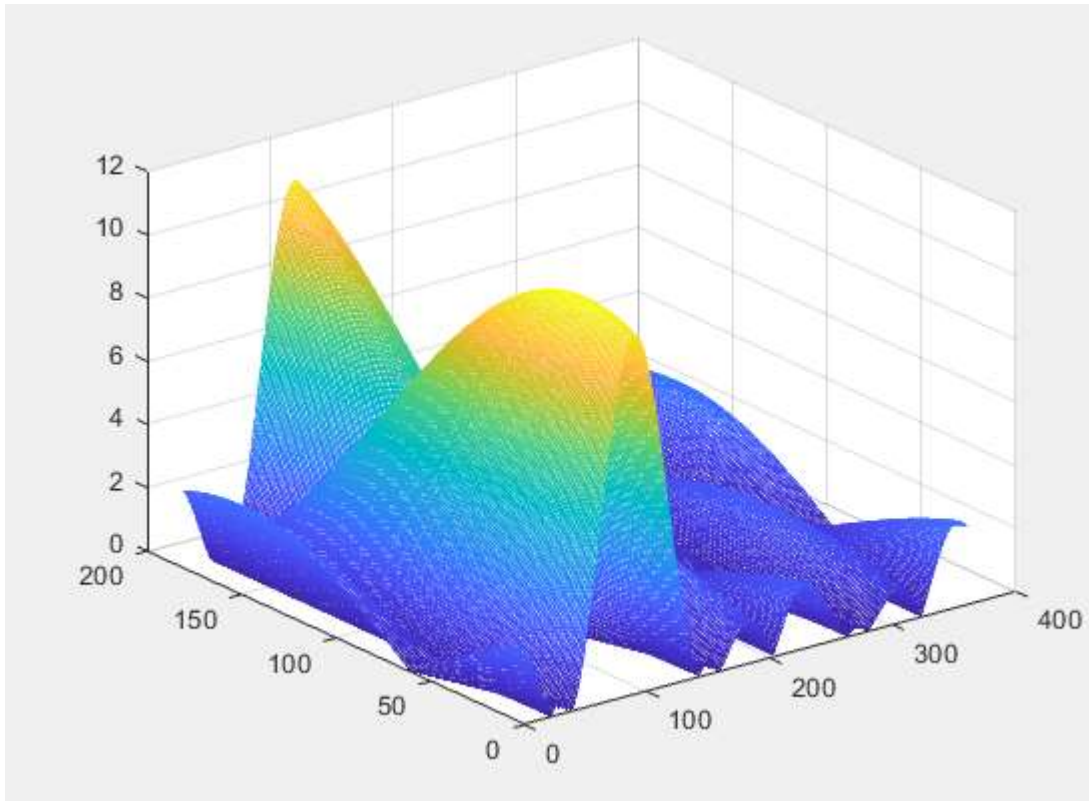
Fig -16: estimated DOA

In 3D location of the target, we could have more precision about the locatization because it uses two angles : azimuth and elevation. In this article, we have predicted two targets. All the response are expressed on degree.

- Target 1 with angulars $(\Phi, \theta) = (100, 50)$

- Target 2 with angulars $(\Phi, \theta) = (100, 200)$

- Target 3 with angulars $(\Phi, \theta) = (80, 200)$

To perform muti-targeting, we also predict the range and speed of each target. The result can be see in Figure 17.

As an interpretation, this Figure shows us the ordinate as the range (m) and his equivalence with the power (dB). We could see the 3 targets at 34m, 38m and 42m.

The speed has a direction and this direction is noted in positive or negative numbers. The target 1 in the Figure has speed at (-1 to 1 m/s); target 2 at (-3 to 1 m/s) and target 3 at (-1 to 1 m/s)
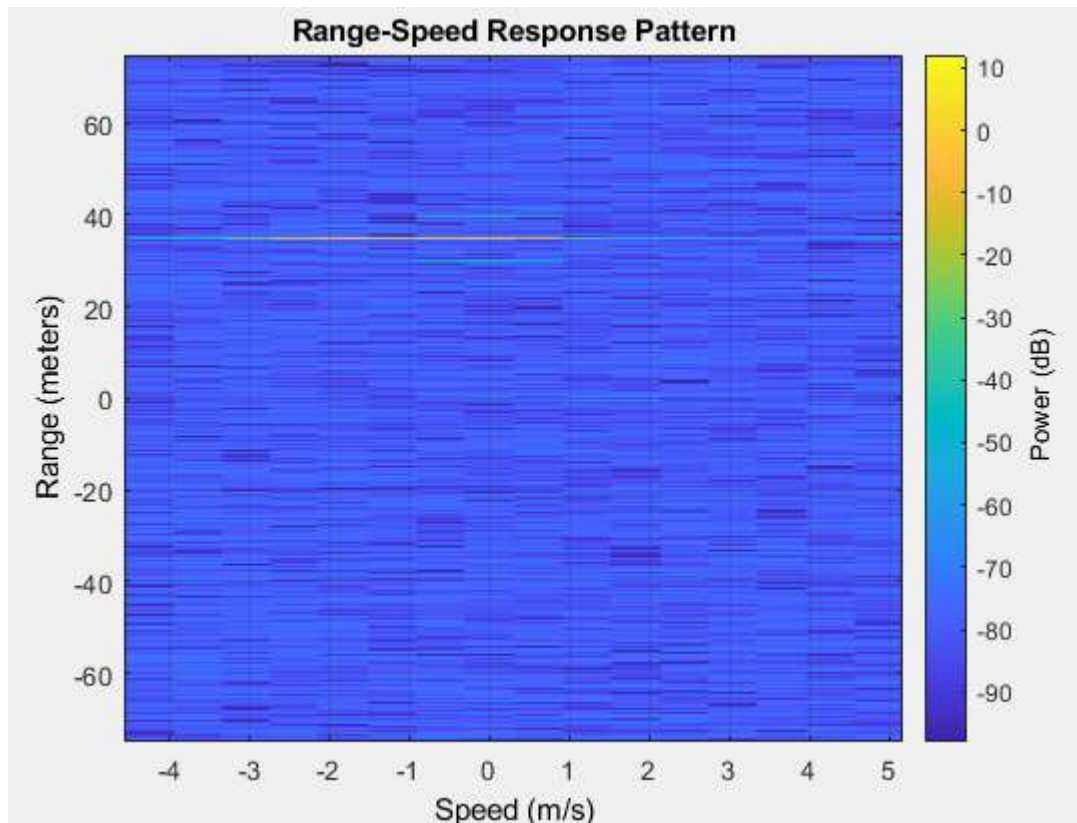
4. CONCLUSIONS

This article shows the feasibility of MIMO RADAR FMCW in 3D with azimuth and elevation estimation not like the classic FMCW. We can predict all interesting information like azimuth, elevation, speed , range, power at dB. Our methods have low complexity, not like MUSIC, Root-MUSIC or ESPRIT estimation. The result has until one meter of precision. Like perspective, we could improve the precision of algorithms using multiple detections.

5. REFERENCES

[1]. D. Patrick, Y. Huang, P.V. Brennan, "FMCW Based MIMO Imaging RADAR", RMMS 2014

[2]. Q. Chen, K. Chetty, P. Brennan, L. B. Lock, M. Ritchie, W. karl, "A coherent through-wall MIMO phased array imaging radar based on time-duplexed switching" SPIE journal 2017

[3]. K. Simon, C. Harun, P. Nils, "A Compact 120 GHz SiGe:C based 2×8 FMCW MIMO Radar Sensor for Robot Navigation in Low Visibility Environments", European Radar Conference 2017

[4]. T. Fickenscher, A. Gupta, J. Hinz, M. Holters, U. Zölzer, "MIMO Surface Wave Radar Using Time Staggered FMCW Chirp Signals", European Radar Conference 2011

[5]. Z. Peterson, "FMCW MIMO Radar Design for Aerospace, Autos, and Robotics", NWES journal 2021

[6]. A. J. Jong, "Orthogonal waveforms for FMCW MIMO radar", IEEE 2011

[7]. J. O. Hinz and U. Z̈olzer, "A MIMO FMCW radar approach to HFSWR", Advances in Radio Science, 2011

[8]. Z. Lu, "A Low-Complexity 2D-DOA Estimation Algorithm with Massive URA", Journal of Physic 2020

[9] Y. Jin, B. Kim, S. Kim, J. Lee, "Design and Implementation of FMCW Surveillance Radar Based on Dual Chirps", ELEKTRONIKA IR ELEKTROTECHNIKA 2018

[10] Y. Jin, B. Kim, S. Kim, J. Lee, "FMCW Radar Estimation Algorithm with High Resolution and Low Complexity Based on Reduced Search Area", MDPI journals 2022